Electronic Supplementary Information (ESI)

A calix[4]resorcinarene-based giant coordination cage: controlled assembly and iodine uptake

Wen-Yuan Pei,[a] Jin Yang,*[a] Hui Wu,[b] Wei Zhou,*[b] Ying-Wei Yang*[c] and Jian-Fang Ma*[a]

[a]*Key Lab for Polyoxometalate Science, Department of Chemistry, Northeast Normal University, Changchun 130024, China*

[b] *NIST Center for Neutron Research, National Institute of Standards and Technology, Gaithersburg, Maryland 20899-6102, United States*

[c]*State Key Laboratory of Inorganic Synthesis and Preparative Chemistry, International Joint Research Laboratory of Nano-Micro Architecture Chemistry (NMAC), College of Chemistry, Jilin University, 2699 Qianjin Street, Changchun 130012, China*

Correspondence to:
yangj808@nenu.edu.cn (J. Yang)
wzhou@nist.gov (W. Zhou)
ywyang@jlu.edu.cn (Y.-W. Yang)
majf247@nenu.edu.cn (J.-F. Ma)

I. Experimental section

Materials and methods. All chemicals were obtained from commercial sources. The C, H, and N elemental analyses were recorded on a vario EL cube elemental analyzer. The FT-IR spectra were measured using KBr pellets on a Mattson Alpha-Centauri spectrometer. X-ray photoelectron spectroscopy (XPS) measurement was conducted on a VG Thermo ESCALAB 250 spectrometer (VG Scientific) operated at 120 W. PXRD patterns were measured on a Rigaku Dmax 2000 X-ray diffractometer with graphite monochromatized CuKα radiation (λ = 0.154 nm). Thermogravimetric (TG) curves were determined on a PerkinElmer TG-7 by heating the sample from 50 to 800 ˚C under nitrogen gas.

The tetra(2-(4H-pyrazol-3-yl)pyridine)calix[4]resorcinarene (*Pen*-TPC4R) was prepared using a method similar to the literature report.[1] The 3,3',5,5'-azobenzene tetracarboxylic acid (H_4TAZB) was purchased from commercial sources.

Single crystal X-ray crystallography. Crystallographic data of **cage-1** was measured on a Bruker D8 VENTURE X-ray diffractometer, using φ and ω scans with MoK_α radiation (λ = 0.71073 Å) at room temperature. The structure of **cage-1** was solved by direct method and refined on F^2 by full-matrix least-squares using the *SHELXTL*-2018 program within WINGX.[2-4] Carbon atoms of partial pentyl groups for **cage-1** were refined isotropically. Hydrogen atoms of carbons were placed geometrically. In the refinements of **cage-1**, the SQUEEZE routine in PLATON was employed to remove the highly disordered solvents.[5] Structural refinement parameters and crystallographic data are given in Table S2.

Synthesis of $[Zn_{24}($*Pen*$-TPC4R)_6(TAZB)_{12}]\cdot 54DMF\cdot 40MeOH\cdot 30H_2O$ (cage-1). A mixture of H_4TAZB (7 mg, 20 mmol), *Pen*-TPC4R (10 mg, 8 mmol), $Zn(NO_3)_2\cdot 6H_2O$ (15 mg, 50 mmol) and DMF/MeOH (8 mL, 3/5, v/v) was added to a Teflon reactor (15 mL) and heated at 110 °C for 3 days. Yellow crystals of **cage-1** were obtained in a *ca.* 44 % yield based on *Pen*-TPC4R. Element analysis (%) for $C_{922}H_{1222}N_{150}O_{268}Zn_{24}$ (**cage-1**): calculated C 54.65, H 6.08, N 10.37; found C 52.14, H 5.80, N 10.56. IR data (KBr cm^{-1}): 3421(w), 2928(m), 2857(m), 1670(s), 1571(m), 1439(s), 1347(s), 1242(m), 1147(w), 1091(m), 1014(w), 983(m), 957(m), 780(m), 731(w), 691(w), 658(w), 584(w), 517(w). CCDC 1843556 contains the supplementary crystallographic data for **cage-1**.

Activation of cage-1. Prior to the I_2 adsorption, the fresh sample of **cage-1** was guest-exchanged with dry acetone over three days. Then the sample was filtered and activated at 60 °C under vacuum for about 10 h. After complete solvent removal, the sample no longer exhibits sharp diffraction peaks in the PXRD data, suggesting that the cage-cage stacking loses long-range order. This loss of crystallinity is most likely due to the giant size of the cage molecule. Importantly, the PXRD peaks and the sample crystallinity can be fully recovered by simply soaking the activated sample in DMF solvent. This demonstrates that the structures of individual cage molecules are well maintained upon sample activation and the loss of long-range order in cage packing is only temporary.

[1] (a) Y. J. Hu, J. Yang, Y. Y. Liu, S. Y. Song and J. F. Ma, *Cryst. Growth Des.* 2015, **15**, 3822. (b) W. Y. Pei, G. H. Xu, J. Yang, H. Wu, B. L. Chen, W. Zhou and J. F. Ma, *J. Am. Chem. Soc.* 2017, **139**, 7648.

[2] G. M. Sheldrick, *SHELXS-2018*, *Program for the crystal structure solution*; University of Göttingen: Göttingen, Germany, **2018**.

[3] G. M. Sheldrick, *SHELXL-**2018***, *Program for the crystal structure refinement*; University of Göttingen: Göttingen, Germany, **2018**.

[4] L. J. Farrugia, *WINGX: A Windows Program for Crystal Structure Analysis*; University of Glasgow: Glasgow, UK, **1988**.

[5] A. L. Spek, *J. Appl. Crystallogr.* 2003, **36**, 7.

II. Supporting figures

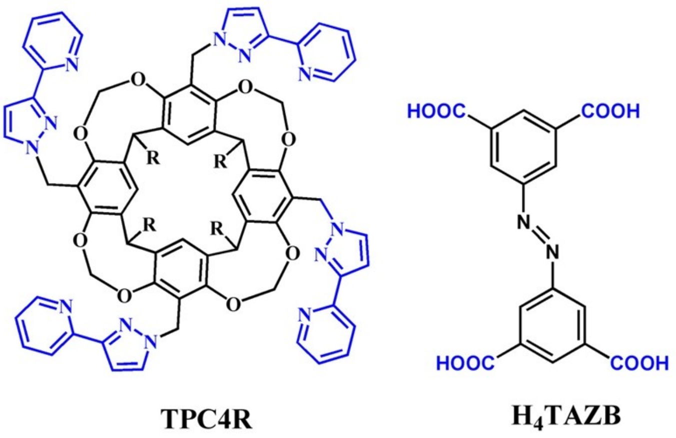

Scheme S1. Calix[4]resorcinarene-based ligand (*Pen*-TPC4R, where R = Pentyl) and rigid aromatic tetracarboxylic acid (H_4TAZB).

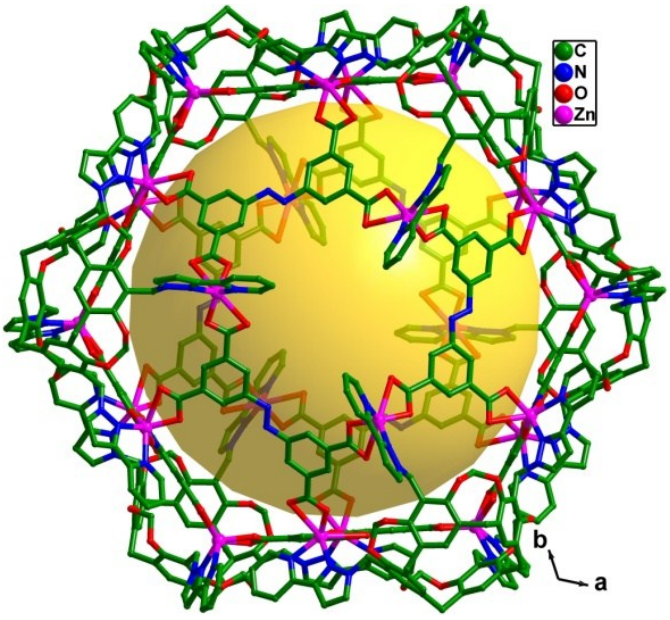

Fig. S1 View of the structure of the giant $\{Zn_{24}\}$ coordination cage of **cage-1** along the *c* axis.

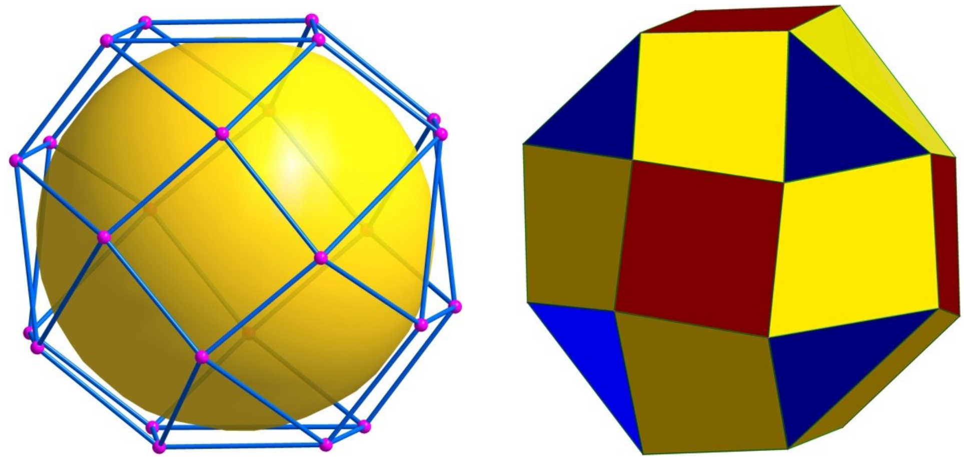

Fig. S2 Schematic representation of the rhombicuboctahedron in **cage-1** when considering the Zn(II) atoms as vertices.

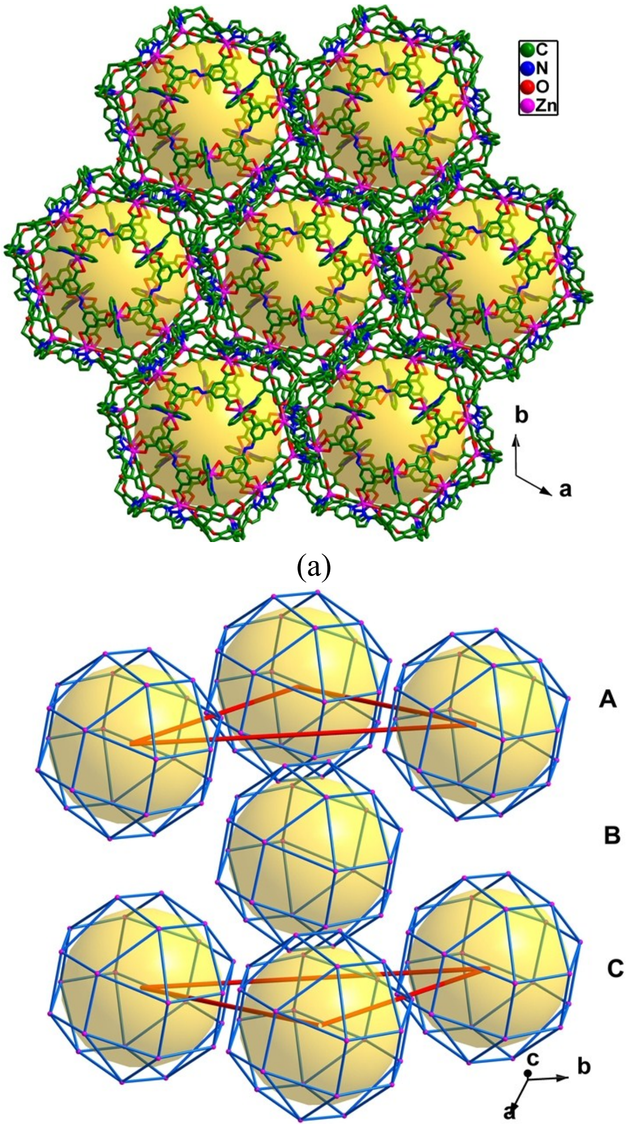

(a)

(b)

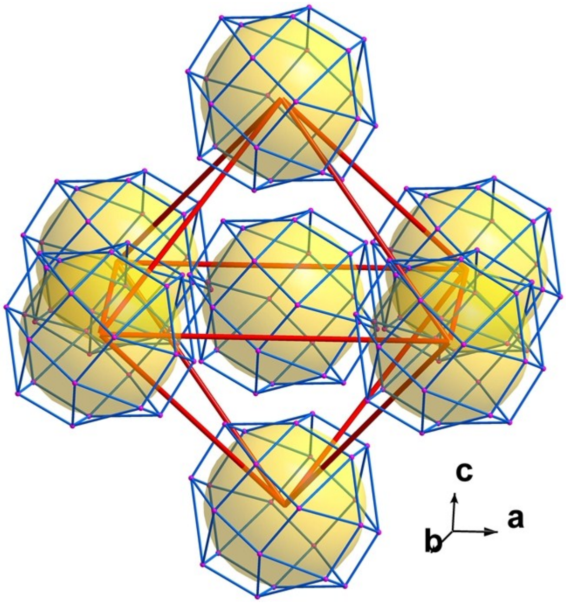

(c)

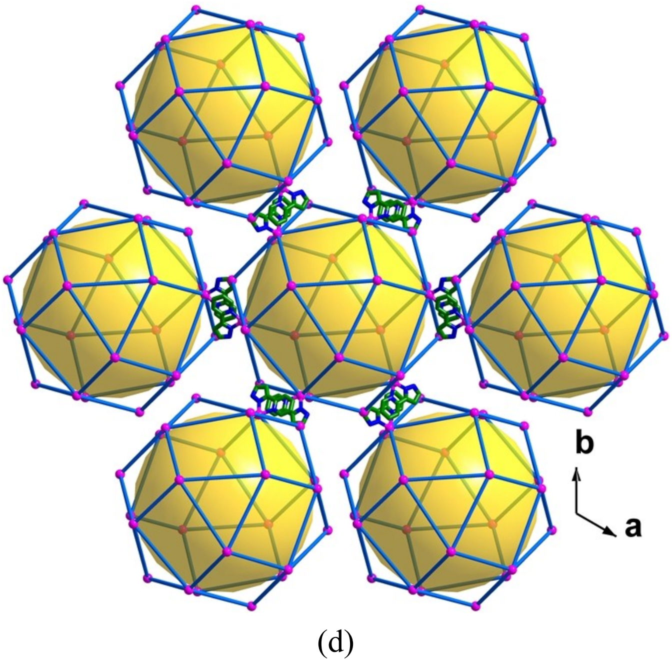

(d)

Fig. S3 (a) View of the hexagonal architecture of **cage-1**. (b) View of each cage surrounded by six nearest-neighbor cages: three from the layer above and three from the layer below. (c) View of the octahedral architecture composed of central cage with six nearest-neighbor cages. (d) Schematic showing the π-π interactions of one cage with its six nearest neighbors in **cage-1**.

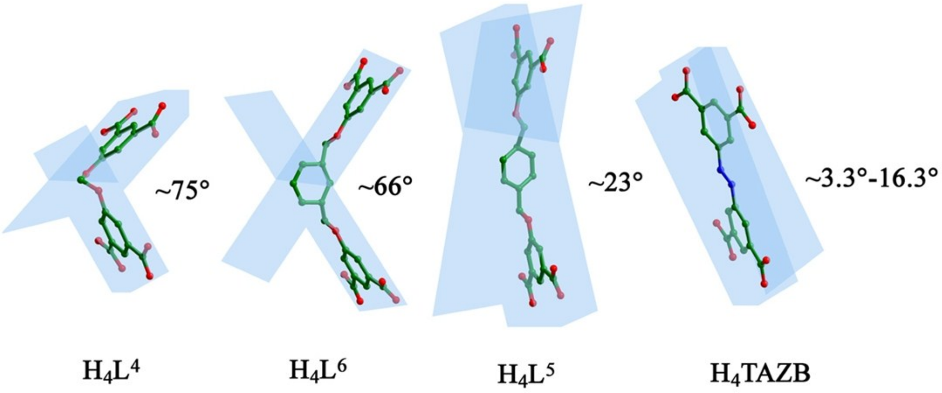

Fig. S4 Schematic diagram of dihedral angles of ancillary flexible tetracarboxylic acids (H_4L^4, H_4L^5 and H_4L^6) and the rigid tetracarboxylic acid (H_4TAZB).

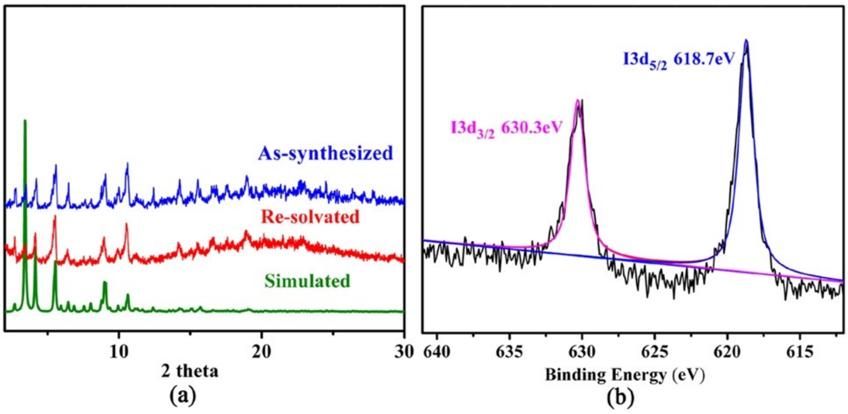

Fig. S5 (a) PXRD patterns of **cage-1**: simulated (green), as-synthesized (blue) and re-solvated one after I_2 adsorption (red). (b) Specific region for I_2 in XPS spectra of I_2 loaded **cage-1**.

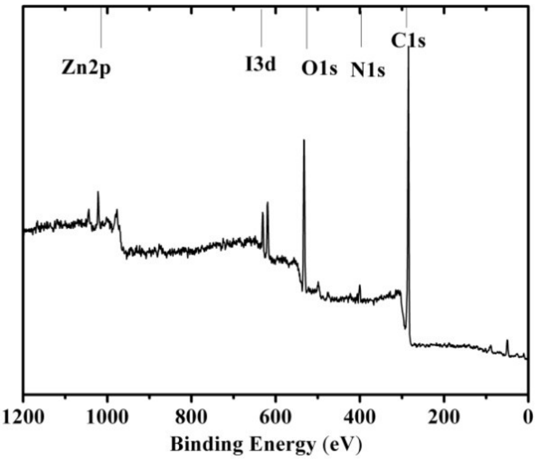

Fig. S6 Full range for I_2 in XPS spectra of I_2 loaded **cage-1**.

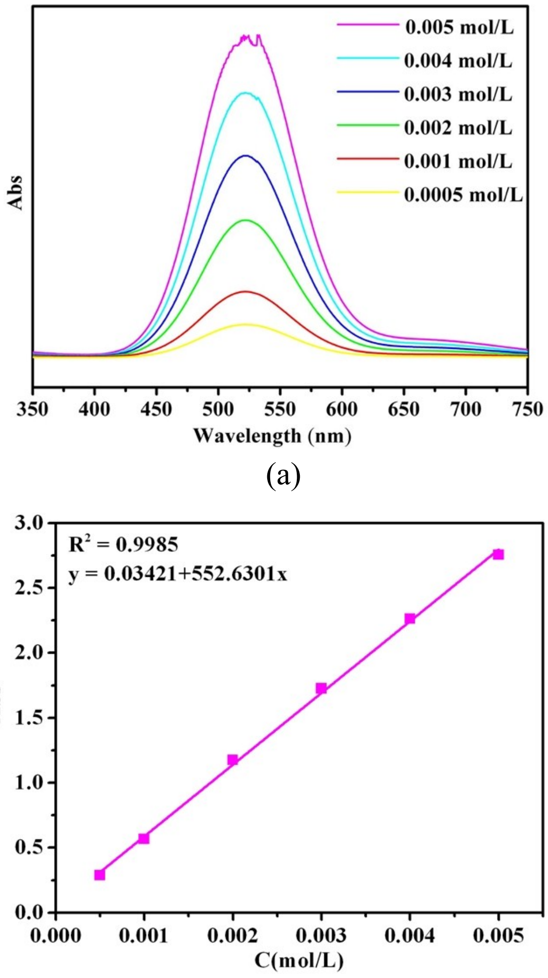

(a)

(b)

Fig. S7 (a) Calibration curve of standard iodine determined by UV-Vis spectra in *n*-hexane solution. (b) The fitting of Abs value *vs* concentration of I_2.

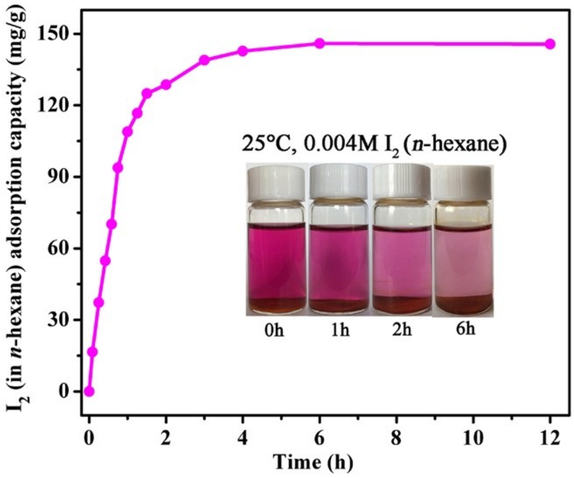

Fig. S8 Iodine uptakes (mg g^{-1}) over time by crystalline sample of **cage-1** in the iodine *n*-hexane solution (The inset shows color changes of the iodine *n*-hexane solutions from purple to light pink with iodine removal by **cage-1**).

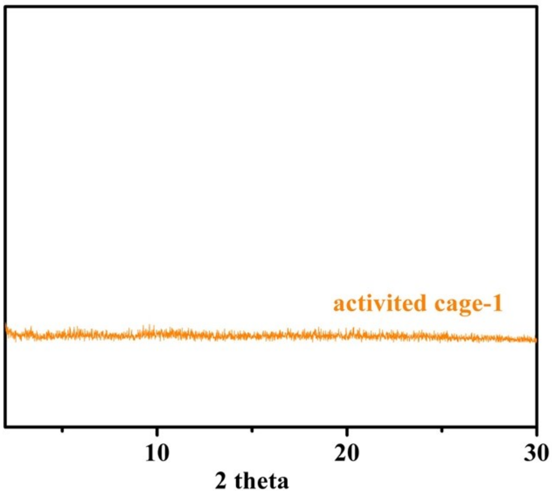

Fig. S9 PXRD pattern for the activated sample of **cage-1.**

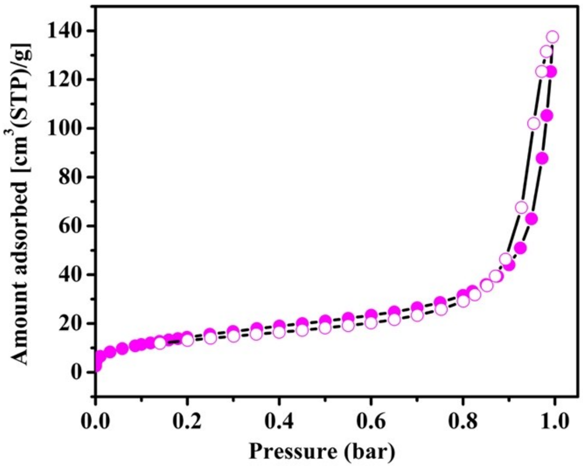

Fig. S10 N_2 adsorption isotherms (77K) for **cage-1** (It becomes amorphous after activation). The N_2 adsorption isotherm of **cage-1** at 77 K shows type-II adsorption behavior. The maximum N_2 uptakes at 77 for **cage-1** is ~137 cm^3·g^{-1}.

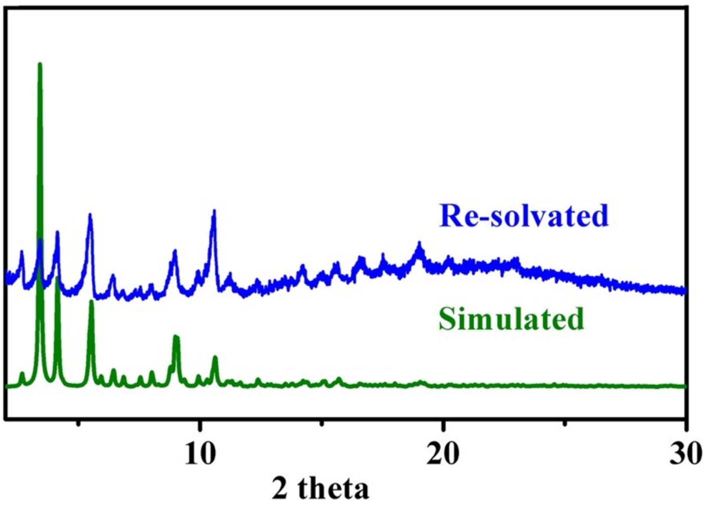

Fig. S11 PXRD patterns of **cage-1:** simulated (green) and re-solvated one after activation (blue).

III. Thermogravimetric analysis.

For **cage-1**, the thermogravimetric curve was determined under nitrogen gas from 50 to 800 ˚C. For **cage-1**, the weight loss of *ca.* 28.5% before 149.8 ˚C can be attributed to the removal of free solvents (54DMF, 40MeOH and 30H_2O). The residual components began to decompose from 350 ˚C.

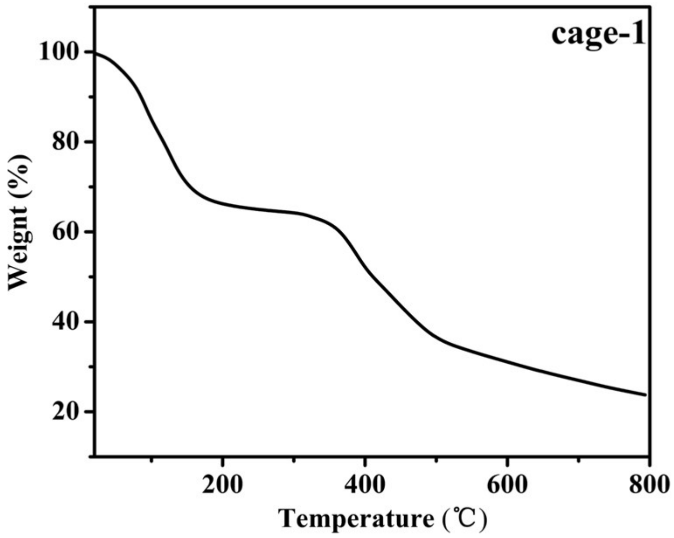

Fig. S12 TG curve of **cage-1.**

IV. IR Spectra.

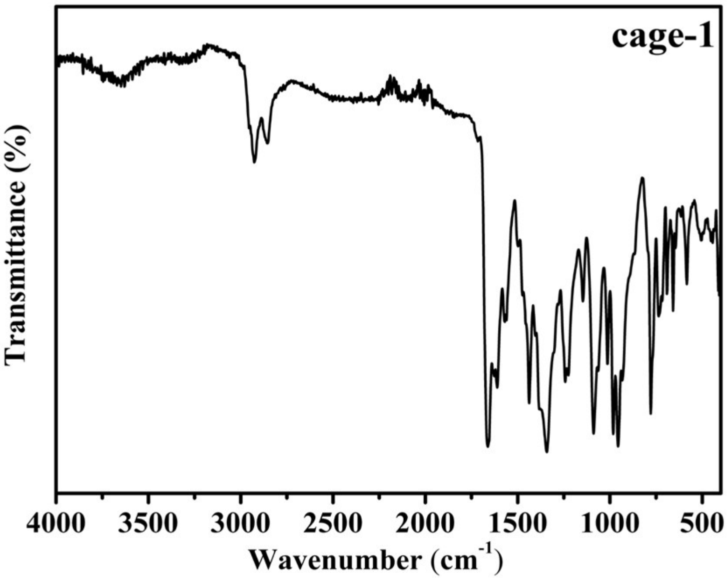

Fig. S13 IR spectra of **cage-1.**

V. Tables

Table S1. Summary of iodine adsorption capacity for typical porous materials.

No.	Adsorbent	Temperature (℃)	Adsorption Capacity (mg/g)	References
1	Cage-1	75	1420	This work
2	Cg-5C	~25a)	239	[1]
3	Cg-5P	~25a)	87	[1]
4	CalP_n (n = 2-4)	75	884-2200	[2]
5	CalP_n-Li (n = 2-4)	75	1083-3120	[2]
6	COP-Series	60	195-380	[3]
7	PAF-n (n = 23-25)	75	2600-2760	[4]
8	ZIF-8	75	1200	[5]
9	MFM-300	80	1540	[6]
10	HKUST-1	75	~1500	[7]
11	JUC-Z2	25	1440	[8]
12	Cu-BTC	75	1750	[9]
13	AgX-silver exchanged faujasite	~150	80-200	[10]
14	AgA-silver impregnated alumina	~150	100-235	[10]
15	Macroreticular resins	<50	200-1000	[10]
16	AgZ-silver exchanged mordenite	~150	~170	[10]

a) At room temperature.

[1] B. J. Riley, J. Chun, J. V. Ryan, J. Matyáš, X. S. Li, D. W. Matson, S. K. Sundaram, D. M. Strachan and J. D. Vienna, *RSC Adv.*, 2011, **1**, 1704.

[2] D. Shetty, J. Raya, D. S. Han, Z. Asfari, J.-C. Olsen and A. Trabolsi, *Chem. Mater.*, 2017, **29**, 8968.

[3] G. Das, T. Prakasam, S. Nuryyeva, D. S. Han, A. Abdel-Wahab, J. C. Olsen, K. Polychronopoulou, C. Platas-Iglesias, F. Ravaux, M. Jouiad and A. Trabolsi, *J. Mater. Chem. A*, 2016, **4**, 15361.

[4] Z. Yan, Y. Yuan, Y. Tian, D. Zhang and G. Zhu, *Angew. Chem. Int. Ed.*, 2015, **54**, 12733.

[5] D. F. Sava, M. A. Rodriguez, K. W. Chapman, P. J. Chupas, J. A. Greathouse, P. S. Crozier and T. M. Nenoff, *J. Am. Chem. Soc.* 2011, **133**, 12398.

[6] X. R. Zhang, I. D. Sliva, H. G. W. Godfrey, S. K. Callear, S. A. Sapchenko, Y. Q. Cheng, I. Vitórica-Yrezábal, M. D. Frogley, G. Cinque, C. C. Tang, C. Giacobbe, C. Dejoie, S. Rudić, A. J. Ramirez-Cuesta, M. A. Denecke, S. H. Yang and M. Schröder, *J. Am. Chem. Soc.* 2017, **139**, 16289.

[7] D. F. Sava, K. W. Chapman, M. A. Rodriguez, J. A. Greathouse, P. S. Crozier, H. Zhao, P. J. Chupas and T. M. Nenoff, *Chem. Mater.* 2013, **25**, 2591.

[8] C. Y. Pei, T. Ben, S. X. Xu and S. L. Qiu, *J. Mater. Chem. A*, 2014, **2**, 7179.

[9] D. F. Sava, K. W. Chapman, M. A. Rodriguez, J. A. Greathouse, P. S. Crozier, H. Y. Zhao, P. J. Chupas and T. M. Nenoff, *Chem. Mater.*, 2013, **25**, 2591.

[10] D. R. Haefner, T. J. Tranter, Methods of Gas Phase Capture of Iodine from Fuel Reprocessing Off-Gas: A Literature Survey, INL/EXT-07-12299, Idaho National Laboratory: Idaho Falls, ID, **2007**.

Table S2. Crystallographic data for **cage-1.**

Compound	**cage-1**
Empirical formula	$C_{922}H_{1222}N_{150}O_{268}Zn_{24}$
Formula weight	20263.30
Temperature (K)	293(2)
Crystal system	Trigonal
Space group	*R*-3
a (Å)	51.4950(14)
b (Å)	51.4950(14)
c (Å)	48.469(3)
α(°)	90
β(°)	90
γ(°)	120
V(Å^3)	111308(9)
Z	3
D_{calc} (g·cm^{-3})	0.907
F(000)	32004
R_{int}	0.0967
GOF on F^2	1.077
R_1, wR_2 [I>2σ(I)]	0.1049, 0.3039
R_1, wR_2 (all data)	0.2286, 0.3981

$^aR_1 = \Sigma||F_o| - |F_c||/\Sigma|F_o|$. $^bwR_2 = \{\Sigma[w(F_o^2-F_c^2)^2]/\Sigma w(F_o^2)^2]\}^{1/2}$

**The formula is based on the contents without the unidentified disordered solvent molecules.*

Table S3. Selected bond distances (Å) and angles (deg) for **cage-1.**

N(2)-Zn(2)	2.044(6)	O(22)$^{\#3}$-Zn(2)-N(2)	124.2(2)
N(3)-Zn(2)	2.139(7)	O(22)$^{\#3}$-Zn(2)-O(10)	115.9(2)
N(5)-Zn(3)	2.046(5)	N(2)-Zn(2)-O(10)	98.9(2)
N(6)-Zn(3)	2.101(5)	O(22)$^{\#3}$-Zn(2)-N(3)	99.2(2)
N(8)-Zn(4)	2.029(6)	N(2)-Zn(2)-N(3)	75.8(2)
N(11)-Zn(1)	2.042(7)	O(10)-Zn(2)-N(3)	139.2(2)
N(12)-Zn(1)	2.091(6)	O(22)$^{\#3}$-Zn(2)-O(9)	108.2(2)
O(9)-Zn(2)	2.329(7)	N(2)-Zn(2)-O(9)	127.4(2)
O(10)-Zn(2)	2.054(6)	O(10)-Zn(2)-O(9)	58.1(2)
O(12)-Zn(3)	1.943(5)	N(3)-Zn(2)-O(9)	92.6(2)
O(14)-Zn(3)	1.965(5)	O(12)-Zn(3)-O(14)	120.3(2)
O(16)-Zn(4)	1.932(5)	O(12)-Zn(3)-N(5)	117.9(2)
O(18)-Zn(4)$^{\#2}$	1.949(5)	O(14)-Zn(3)-N(5)	101.1(2)
O(20)-Zn(1)$^{\#2}$	1.960(5)	O(12)-Zn(3)-N(6)	101.1(2)
O(22)-Zn(2)$^{\#1}$	1.955(5)	O(14)-Zn(3)-N(6)	131.2(2)
O(23)-Zn(1)$^{\#1}$	1.942(6)	N(5)-Zn(3)-N(6)	78.5(2)
O(23)$^{\#3}$-Zn(1)-O(20)$^{\#4}$	115.7(2)	O(16)-Zn(4)-O(18)$^{\#4}$	121.5(3)
O(23$^{)\#3}$-Zn(1)-N(11)	102.2(2)	O(16)-Zn(4)-N(8)	119.4(2)
O(20)$^{\#4}$-Zn(1)-N(11)	125.0(3)	O(18)$^{\#4}$-Zn(4)-N(8)	101.5(3)
O(23)$^{\#3}$-Zn(1)-N(12)	133.4(2)	O(16)-Zn(4)-N(9)	103.3(3)
O(20)$^{\#4}$-Zn(1)-N(12)	99.4(3)	O(18)$^{\#4}$-Zn(4)-N(9)	126.3(3)
N(11)-Zn(1)-N(12)	79.0(3)	N(8)-Zn(4)-N(9)	77.5(3)
O(23)$^{\#3}$-Zn(1)-C(104)$^{\#3}$	27.4(2)	O(16)-Zn(4)-C(119)$^{\#4}$	113.6(3)
O(20)$^{\#4}$-Zn(1)-C(104)$^{\#3}$	108.3(3)	O(18)$^{\#4}$-Zn(4)-C(119)$^{\#4}$	29.4(3)
N(11)-Zn(1)-C(104)$^{\#3}$	122.5(3)	N(8)-Zn(4)-C(119)$^{\#4}$	123.6(3)
N(12)-Zn(1)-C(104)$^{\#3}$	114.5(3)	N(9)-Zn(4)-C(119)$^{\#4}$	108.3(3)

Symmetry transformations used to generate equivalent atoms: $^{\#1}$*y+1,-x+y+1,-z+1;* $^{\#2}$ *-x+y+2,-x+1; z* $^{\#3}$ *x-y,x-1,-z+1;* $^{\#4}$ *-y+1, x-y-1, z.*